Single Charged Pion Photoproduction from the Nucleon at 11 GeV

July 7, 2006

W. Chen, D. Dutta, H. Gao(Spokesperson), K. Kramer, X. Qian, Q. Ye, X.F. Zhu, X. Zong
DUKE UNIVERSITY

J. Dunne, D. Dutta(Spokesperson),
MISSISSIPPI STATE UNIVERSITY

J. Arrington, K. Hafidi, D.F. Geesaman, R.J. Holt(Spokesperson), D. H. Potterveld, P. E. Reimer, P. Solvignon
ARGONNE NATIONAL LABORATORY

T. Averett, V. Sulkosky
COLLEGE OF WILLIAM and MARY

C. Glashausser, R. Gilman, X.D. Jiang, G. Kumbartzki, R.D. Ransome, E. C. Schulte
RUTGERS UNIVERSITY

Z.-E. Meziani
TEMPLE UNIVERSITY

A. Bruell, P.Bosted, J.P. Chen, R. Ent, D. Gaskell, D. Mack, T. Horn
THOMAS JEFFERSON NATIONAL ACCELERATOR FACILITY

E.R. Kinney
UNIVERSITY OF COLORADO

E. J. Beise, H. Breuer
UNIVERSITY OF MARYLAND

Abstract

The $\gamma n \to \pi^- p$ and $\gamma p \to \pi^+ n$ reactions are essential and simplest probes of the transition from meson-nucleon degrees of freedom to quark-gluon degrees of freedom in exclusive processes. The cross sections of these processes are also advantageous, for detailed investigation of the possible oscillatory scaling behavior around the (generalized) quark counting rule prediction, since they decrease relatively slower with energy compared with other photon-induced processes. We propose to perform singles $\gamma p \to \pi^+ n$ measurement from hydrogen, and coincidence $\gamma n \to \pi^- p$ differential cross section measurements at the quasi-free kinematics from deuterium for photon energies between 4.4 GeV to 11 GeV at pion center-of-mass angles of $30^\circ < \theta_{CM} < 150^\circ$. Four different energy settings are needed which can be achieved with just one linac energy and four different passes. The proposed measurements will be carried out in Hall C using a 50 μA electron beam impinging on a 6% copper radiator, liquid hydrogen and deuterium targets, and the HMS and the SHMS spectrometers. The 11 GeV CEBAF beam allows for the crossing of the J/Ψ threshold. Therefore, the proposed measurement will provide test of the prediction involving the opening of a new $uuduudc\bar{c}$ resonance state in explaining the well-known oscillatory scaling behavior in the proton-proton elastic scattering data, and to provide detailed investigation of the scaling onset and the underlying mechanism governing the onset of the scaling in photopion production.

Contents

1 Technical Participation of Research Groups

1.1 Argonne National Lab

One spokesperson is from the Argonne National Lab group. The Argonne group will be responsible for the initial optics design of the SHMS. They will also map the field and perform optics verification and commissioning of the SHMS magnets.

1.2 Mississippi State University

Another spokesperson is part of the Mississippi State University group. The MSU groups intends to take responsibility for the design and construction of the collimator and sieve-slit mechanism for the SHMS spectrometer and develop the TRD detector program (not part of baseline equipment) for the SHMS.

2 Introduction

Exclusive processes are essential to studies of transitions from the non-perturbative to perturbative regime of QCD. The differential cross sections for many exclusive reactions [2] at high energy and large momentum transfer appear to obey the quark counting rule [3]. The quark counting rule was originally obtained based on dimensional analysis of typical renormalizable theories. The same rule was later obtained in a short-distance perturbative QCD approach by Brodsky and Lepage[4]. Despite many successes, a model-independent test of the approach, called the hadron helicity conservation rule, tends not to agree with data in the similar energy and momentum region. It has been suggested that contributions from nonzero parton orbital angular momentum could break the hadron helicity conservation rule [5], although these contributions are power suppressed as shown by Lepage and Brodsky [4]. In addition some of the cross-section data can also be explained in terms of non-perturbative calculations [6]. Some recent developments, such as the generalized counting rule proposed by Ji *et al.* [7], the derivation of the quark-counting rule from the anti-de Sitter/Conformal Field Theory (AdS/CFT) correspondence [8], and the machinery to compute the hadronic light front wave functions developed by Brodsky *et al.* [9], have focused interest back on this subject.

In recent years, a renewed trend has been observed in deuteron photo-disintegration experiments at SLAC and JLab [10] - [13]. Onset of the scaling behavior has been observed in deuteron photo-disintegration [12, 13] at a surprisingly low momentum transfer of 1.0 $(\mathrm{GeV/c})^2$ to the nucleon. However, a polarization measurement on deuteron photo-disintegration [14] and in neutral pion photo-production [15], which were recently carried out in Hall A at Jefferson Lab (JLab), shows disagreement with hadron helicity conservation in the same kinematic region where the quark counting behavior is apparently observed. These paradoxes make it essential to understand the exact mechanism governing the early onset of scaling behavior.

Towards this goal, it is important to look closely at claims of agreement between the differential cross section data and the quark counting prediction. Historically, the elastic proton-proton (pp) scattering at high energy and large momentum transfer has played a

very important role. In fact, the re-scaled 90° center-of-mass pp elastic scattering data, $s^{10}\frac{d\sigma}{dt}$ show substantial oscillations about the power law behavior. Oscillations may not be restricted to the pp sector; they are also seen in πp fixed angle scattering [16]; the old [1, 17] as well as the new data [18] (from JLab experiment E94-104) on photo production of charged pions, at $\theta_{cms} = 90°$ also show hints of oscillation about the s^{-7} scaling; see for example Fig. 1. Thus, it is essential to confirm and map out these oscillatory scaling behavior. Using high luminosity and energy upgraded CEBAF, these oscillatory scaling behavior can be investigated with precision to help identify the exact nature and the underlying mechanism responsible for the scaling behavior. For example, is it caused by the quark orbital angular momentum effect seen in the generalized quark counting rule [7] or due to the opening of new charm resonance states [19]? The 11 GeV CEBAF allows one to cross such a charm threshold.

In this experiment, we propose to measure the differential cross-section $\frac{d\sigma}{dt}$ for the $p(\gamma, \pi^+)n$ and $n(\gamma, \pi^- p)$ (using a deuterium target) processes over a range of center-of-mass angles in a photon energy between 5.8 and 11 GeV. Further, single charged pion photoproduction differential cross-section ratio can be formed from these measurements.

The rest of the proposal is organized as following. Section II contains the physics motivations of the proposed measurement, Section III describes the proposed measurement, Section IV contains detailed discussion of the experiment and the beam time request, Section V talks about the collaboration backgrounds and responsibilities and Section VI is the summary.

3 Physics Motivations

3.1 Constituent Counting Rule

The constituent counting rule predicts the energy dependence of the differential cross section at fixed center-of-mass angle for an exclusive two-body reaction at high energy and large momentum transfer as follows:

$$d\sigma/dt = h(\theta_{cm})/s^{n-2}, \tag{1}$$

where s and t are the Mandelstam variables, s is the square of the total energy in the center-of-mass frame and t is the momentum transfer squared in the s channel. The quantity n is the total number of elementary fields in the initial and final states, while $h(\theta_{cm})$ depends on details of the dynamics of the process. In the case of pion photoproduction from a nucleon target, the quark counting rule predicts a s^{-7} scaling behavior for $\frac{d\sigma}{dt}$ at a fixed center-of-mass angle.

The quark counting rule was originally obtained based on dimensional analysis under the assumptions that the only scales in the system are momenta and that composite hadrons can be replaced by point-like constituents. Implicit in these assumptions is the approximation that the class of diagrams, which represent on-shell independent scattering of pairs of constituent quarks (Landshoff diagrams) [27], can be neglected. Also neglected were contributions from quark orbital angular momentum, which are power suppressed but can give rise to hadron helicity flipping amplitudes. These counting rules were also

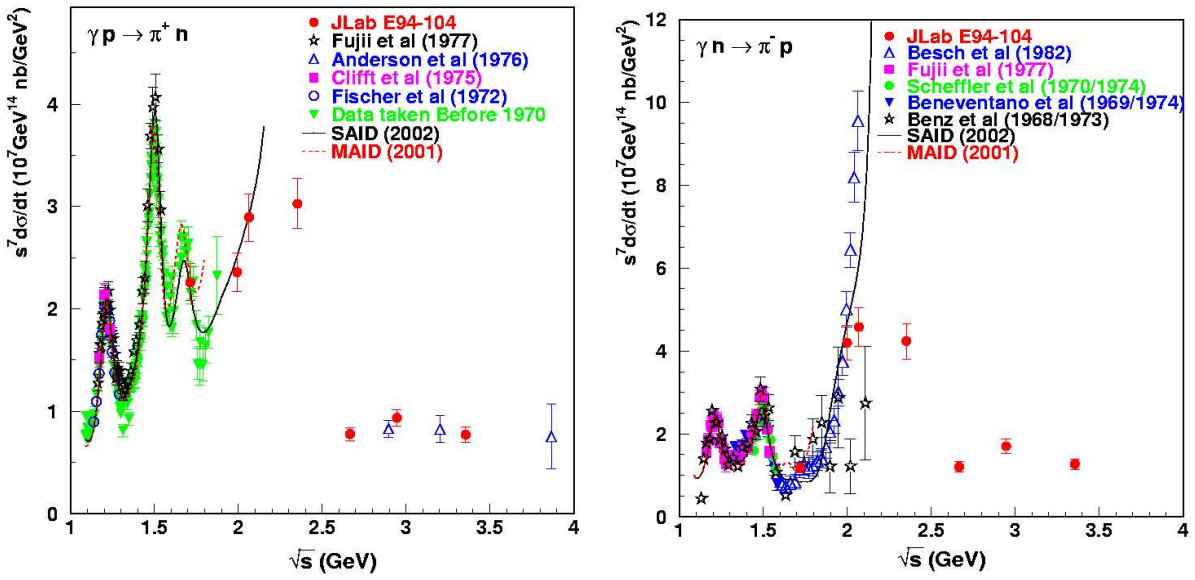

Figure 1: The scaled differential cross section, $s^7 \frac{d\sigma}{dt}$ as a function of $\sqrt{s}$ at a center-of-mass angle of 90° for $\gamma p \to \pi^+ n$ channel (left) and the $\gamma n \to \pi^- p$ channel (right). The data from JLab E94-104 are shown as solid circles. The error bars for the new data and for the Anderson *et al.* data [1], include statistical and systematic uncertainties. Other data sets [17, 20] are shown with only statistical errors. The open squares (right panel) were averaged from data at $\theta_{cm} = 85°$ and 95° [21]. The solid line was obtained from the recent partial-wave analysis of single-pion photoproduction data [22] up to E_γ=2 GeV, while the dashed line from the MAID analysis [23] up to E_γ=1.25 GeV.

confirmed within the framework of perturbative QCD analysis up to a logarithmic factor of α_s and are believed to be valid at high energy, in the perturbative QCD region. Such analysis relies on the factorization of the exclusive process into a hard scattering amplitude and a soft quark amplitude inside the hadron. In the last few years an all-orders demonstration of the counting rules for hard exclusive processes has been shown to arise from the correspondence between the anti-de Sitter space and conformal field theory [8] which connects superstring theory to superconformal gauge theory.

Many exclusive reactions [2, 1] at high energy and large momentum transfer appear to obey the CCR. In recent years, a similar trend, i.e. global scaling behavior, has been observed in deuteron photo-disintegration experiments [11, 12, 13] and in photo-production of charged pions [18] at a surprisingly low transverse momentum value of $\sim$ 1.1 $(\mathrm{GeV/c})^2$. The other natural consequence of pQCD: the helicity conservation selection rule, tends not to agree with data in the experimentally tested region. Hadron helicity conservation arises from quark helicity conservation at high energies and the vector gluon-quark coupling nature of QCD and by neglecting the higher orbital angular momentum states of quarks or gluons in hadrons. The same dimensional analysis which predicts the quark counting rule also predicts hadron helicity conservation for exclusive processes at high energy and large momentum transfers. If hadron helicity conservation holds, the induced polarization of the recoil proton in the unpolarized deuteron photo-disintegration process is expected to be zero. A polarization measurement [14] in deuteron photo-disintegration has been carried out recently by the JLab E89-019 collaboration. While the induced polarization does seem to approach zero around a photon energy of 1.0 GeV at 90° center-of-mass angle, the polarization transfer data are inconsistent with hadron helicity conservation.

The entire subject is very controversial. Isgur and Llewellyn-Smith [6] argue that if the nucleon wave-function has significant strength at low transverse quark momenta ($k_\perp$), then the hard gluon exchange (essential to the perturbative approach) which redistributes the transfered momentum among the quarks, is no longer required. The applicability of perturbative techniques at these low momentum transfers is in serious question. There are no definitive answers to the question- *what is the energy threshold at which pQCD can be applied?* Indeed the exact mechanism governing the observed quark counting rule behavior remains a mystery.

Apart from the early onset of scaling and the disagreement with hadron helicity conservation rule, several other striking phenomena have been observed in *pp* elastic scattering. One such phenomena is the oscillation of the differential cross-section about the scaling behavior predicted by the quark counting rule (s^{-10} for *pp* scattering), first pointed out by Hendry [28] in 1973. Secondly, the spin correlation experiment in *pp* scattering first carried out at Argonne by Crabb *et al.* [29] shows striking behavior: it is ~ 4 times more likely for protons to scatter when their spins are both parallel and normal to the scattering plane than when they are anti-parallel, at the largest momentum transfers ($p_T{}^2 = 5.09$ $(\mathrm{GeV/c})^2$, $\theta_{c.m.} = 90°$). Later spin-correlation experiments [30] confirm the early observation by Crabb *et al.* [29] and showed that the spin correlation A_{NN} (given by $\frac{\sigma(\uparrow,\uparrow)-\sigma(\uparrow,\downarrow)}{\sigma(\uparrow,\uparrow)+\sigma(\uparrow,\downarrow)}$) varies with energy about the pQCD prediction.

Theoretical interpretation of this oscillatory behavior of the scaled cross-section ($s^{10}\frac{d\sigma}{dt}$) and the striking spin-correlation in *pp* scattering was attempted by Brodsky, Carlson, and

Lipkin [31] within the framework of quantum chromodynamic quark and gluon interactions, where interference between hard pQCD short-distance and long-distance (Landshoff) amplitudes was discussed for the first time. The Landshoff amplitude arises due to multiple independent scattering between quark pairs in different hadrons. Although each scattering process is itself a short distance process, different independent scatterings can be far apart, limited only by the hadron size. Moreover, gluonic radiative corrections give rise to a phase to this amplitude which is calculable in pQCD [32]. This effect is believed to be analogous to the coulomb-nuclear interference that is observed in low-energy charged-particle scattering. It was also shown that at medium energies this phase (and thus the oscillation) is energy dependent [33], while becoming energy independent at asymptotically high energies [33], [34]. Carlson, Chachkhunashvili, and Myhrer [38] have also applied such an interference concept to the *pp* scattering and have explained the *pp* polarization data. On the other hand Brodsky and de Teramond [19] have suggested that the structure seen in $s^{10}\frac{d\sigma}{dt}(pp \to pp)$, the A_{NN} spin correlation at $\sqrt{s} \sim 5$ GeV (around center-of-mass angle of 90°) [29],[30] can be attributed to $c\bar{c}uuduud$ resonant states. The opening of this channel gives rise to an amplitude with a phase shift similar to that predicted for gluonic radiative corrections.

3.2 New developments and Generalized counting rule

A number of new developments have generated renewed interest in this topic. Zhao and Close [39] have argued that a breakdown in the locality of quark-hadron duality (dubbed as "restricted locality" of quark-hadron duality) results in oscillations around the scaling curves predicted by the counting rule. They explain that the smooth behavior of the scaling laws arise due to destructive interference between various intermediate resonance states in exclusive processes at high energies, however at lower energies this cancellation due to destructive interference breaks down locally and gives rise to oscillations about the smooth behavior.

On the other hand, Ji *et al.* [7] have derived a generalized counting rule based on pQCD analysis, by systematically enumerating the Fock components of a hadronic light-cone wave function. Their generalized counting rule for hard exclusive processes include parton orbital angular momentum and hadron helicity flip, thus they provide the scaling behavior of the helicity flipping amplitudes. The interference between the different helicity flip and non-flip amplitudes offers a new mechanism to explain the oscillations in the scaling cross-sections and spin correlations. Brodsky *et al.* [9] have used the anti-de Sitter/Conformal Field Theory correspondence or string/gauge duality [8] to compute the hadronic light front wave functions exactly and it yields an equivalent generalized counting rule without the use of perturbative theory. In a further test of these new approaches, calculations of the nucleon formfactors including quark orbital angular momentum in pQCD [40] and those computed from light-front hadron dynamics [9] both seem to explain the $\frac{1}{Q^2}$ fall-off of the proton formfactor ratio, $G_E(Q^2)/G_M(Q^2)$, measured recently at JLab in polarization transfer experiments [41].

We have examined [42] the role of the helicity flipping amplitudes in the oscillatory scaling behavior of *pp* scattering and the oscillations in the spin correlations observed in polarized *pp* scattering. We noticed that just using the Landshoff amplitude and its

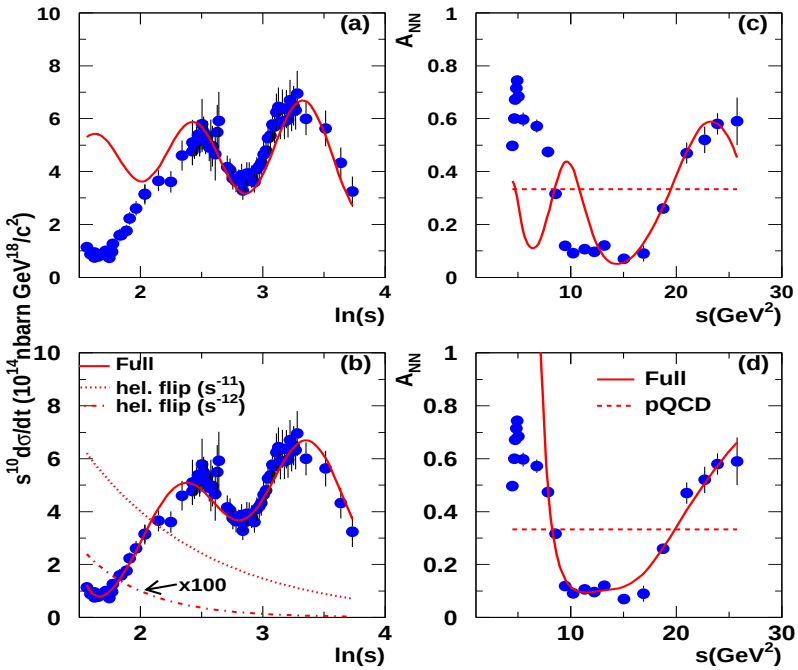

Figure 2: (a) The fit to pp scattering data at $\theta_{cm} = 90°$ of Ralston and Pire [37]. (b) Fit The same data when the helicity flipping amplitudes are included. The solid line is the fit result, the dotted line is contribution from the helicity flip term $\sim s^{-11}$, the dot-dashed line is contribution from the helicity flip term $\sim s^{-12}$. The $\sim s^{-12}$ contribution has been multiplied by 100 for display purposes. (c) The fit to A_{NN} from polarized pp scattering data at $\theta_{cm} = 90°$ of Carlson *et al.* [38]. (d) Fit to the same data when the helicity flip amplitudes are included. The cross-section data are from Ref. [43] and the A_{NN} data are from Ref. [29, 30].

interference with the short distance term, fails to describe the data at low energies ($s < 10$ GeV^2). Since the Landshoff amplitude is expected to be significant only at high energies, it is not unreasonable that the above formalism does not describe the data at low energies. We used the generalized counting rule of Ji *et al.* [7] to obtain the scaling behavior of the helicity flipping amplitudes. Our new fit [42] including the helicity flip amplitudes describes the scaled cross-section as well as the spin-correlation data much better specially at the low energies(Fig. 2). The helicity flip amplitudes arising from the parton orbital angular momentum are non-negligible when the parton transverse momentum can not be neglected compared with the typical momentum scale in the exclusive processes. At relatively low energies this is certainly the case, and thus one would expect the helicity flip amplitudes to be a significant contribution to the cross-section at low energies. Moreover, the generalized counting rule of Ji *et al.* predicts a much faster fall-off with energy for the helicity flip amplitudes as expected. An examination of the explicit contribution from the different amplitudes show that the helicity flip amplitudes and their interference are indeed quite significant at low energies and help describe the data at low energies. Results from our fits are shown in Fig. 2. These are very promising results and should be examined for other reactions.

3.3 Is oscillatory scaling behavior unique to proton-proton elastic scattering?

It was previously thought that the oscillatory $s^{10}\frac{d\sigma}{dt}$ feature is unique to pp scattering or to hadron induced exclusive processes. However, it has been suggested that similar oscillations should occur in deuteron photo-disintegration [44], and photo-pion productions at large angles [45]. The QCD re-scattering calculation of the deuteron photo-disintegration process by Frankfurt, Miller, Sargsian and Strikman [44] predicts that the additional energy dependence of the differential cross-section, beyond the $s^{11}\frac{d\sigma}{dt}$ scaling arises primarily from the $n-p$ scattering in the final state. If these predictions are correct, such oscillatory behavior may be a general feature of high energy exclusive photoreactions. Thus it is very important to experimentally search for these oscillations in photoreactions.

Farrar, Sterman and Zhang [46] have shown that the Landshoff contributions are suppressed at leading-order in large-angle photoproduction but they can contribute at subleading order in $\frac{1}{Q}$ as pointed out by the same authors. In principle, the fluctuation of a photon into a $q\bar{q}$ in the initial state can also contribute an independent scattering amplitude at sub-leading order. However, the vector-meson dominance diffractive mechanism is already suppressed in vector meson photoproduction at large values of t [47]. On the other hand such independent scattering amplitude can contribute in the final state if more than one hadron exist in the final state, which is the case for both the deuteron photo-disintegration and nucleon photo-pion production reactions. Thus, an unambiguous observation of such an oscillatory behavior in exclusive photoreactions with hadrons in the final state at large t may provide a signature of QCD final state interaction. The most recent data on $d(\gamma, p)n$ reaction [12, 13] show that the oscillations, if present, are very weak in this process, and the rapid drop of the cross section ($\frac{d\sigma}{dt} \propto \frac{1}{s^{11}}$) makes it impractical to investigate such oscillatory behavior.

Given that the nucleon photo-pion production has a much larger cross-section at high

energies ($\frac{d\sigma}{dt} \propto \frac{1}{s^7}$), it is very desirable to use these reactions to verify the existence of such oscillations. In fact some precision data on $\gamma p \to \pi^+ n$ and $\gamma n \to \pi^- p$ was recently reported by JLab experiment E94-104 [18]. The results indicate the constituent counting rule behavior at center-of-mass angle of 90°, for photon energies above ~ 3 GeV (i.e. above the resonance region). In addition to the s^{-7} scaling behavior, these data also suggest an oscillatory behavior. However, the rather coarse beam energy settings prevent a conclusive statement about the oscillatory behavior. Moreover, the photo-pion production data can also be described similarly by including the helicity flip terms along with the Landshoff terms [42], however because of the coarse energy spacing of the data the results of these new fits are not as illustrative as the *pp* case. The present proposed measurements are exploratory over relatively coarse energy intervals to verify scaling, to search for further evidence of oscillations, to test the simple factorization model of Huang and Kroll in the pi-/pi+ ratio and to further assess the value of a possible future experiment with a finer energy scan.

3.4 Single charged pion production ratio from nucleon at large momentum transfers

An earlier onset to the scaling associated with pQCD may be seen by forming ratios of differential cross sections from exclusive processes. The simplest of such ratios is the charged pion photoproduction differential cross-section ratio, $\frac{d\sigma}{dt}(\gamma n \to \pi^- p)/\frac{d\sigma}{dt}(\gamma p \to \pi^+ n)$.

In such a ratio, non-perturbative effects may cancel and one may expect the π^-/π^+ ratio to give the first indication of the onset of pQCD. Calculations of this ratio have been carried out in the framework of handbag mechanism [24, 25], in which the amplitude is factorized into a parton-level subprocess $\gamma q_a \to P q_b$ and generalized parton distributions (GPD). The GPD part of the contribution describing the soft hadron-parton transitions indeed cancels in this ratio provided the assumption of negligible quark helicity flip contributions and the dominance of a particular helicity conserving gauge invariant covariant describing the amplitude of the parton-level subprocess $\gamma q_a \to P q_b$ for pseudoscalar meson production [25]. The most recent charged pion ratio data [18] from experiment E94-104 for momentum transfers up to 5.0 $(\mathrm{GeV/c})^2$ suggest that indeed one of the helicity conserving gauge invariant covariants dominates. This ratio measurement can be extended to a $|t|$ value of about 10 $(\mathrm{GeV/c})^2$, significantly higher than the projected Q^2 value of 6.0 $(\mathrm{GeV/c})^2$ for the charged pion form factor measurement with a 11 GeV beam.

3.5 Summary

The $\gamma p \to \pi^+ n$ and the $\gamma n \to \pi^- p$ processes are the simplest exclusive processes to investigate the transition from the nucleon-meson degrees of freedom to the quark-gluon degrees of freedom of QCD utilizing fully the advantages of high luminosity and the energy upgraded CEBAF. The slower decrease of the differential cross-section for the process compared with many other photon induced two-body processes allows differential cross-section measurements all the way to the highest possible center-of-mass energy with a 11 GeV CEBAF beam. Specifically, a 11 GeV beam will allow:

1. Detailed investigation of the angular dependent scaling onset as observed in the deuteron photodisintegration process and to understand the origin of scaling behavior.

2. Study of the ratio of the differential cross-sections for the charged pion photoproduction from nucleons as a function of momentum transfer to test the transition from non-perturbative to perturbative QCD. This ratio can be extended to significantly higher momentum transfered squared ($|t| \sim 11$ (GeV/c)^2), compared to the proposed pion form-factor ($Q^2 \sim 6$ (GeV/c)^2)experiment.

3. Tests of generalized quark counting rule prediction and to investigate indirectly the effect of quark orbital angular momentum.

4. Search for oscillatory scaling behavior as shown in the proton-proton elastic scattering data and was suggested possibly by the E94-104 results [18].

5. Test predictions of the origin of such oscillatory scaling behavior if observed because the 11 GeV photon beam will allow for the crossing of the charm production threshold.

In this proposal we plan to investigate the **first 2 points** summarized above, a more detailed investigation to address $\mathbf{3-5}$ would follow after a successful completion of this proposed experiment.

4 Proposed Measurements

We propose to carry out a measurement of the photo-pion production cross-section for the fundamental $\gamma n \rightarrow \pi^- p$ process from a ^{2}H target and for the $\gamma p \rightarrow \pi^+ n$ process from a hydrogen target over pion center-of-mass angle ranging between $30^o < \theta_{CM} < 150^o$, and $\sqrt{s}$ over a range of 3.0 GeV to 4.62 GeV. The maximum beam energy requested is 11 GeV, in addition three other energies are requested, however they do not require any changes in the linac energy. We plan to make individual cross-section measurements with a 3% statistical uncertainty and point-to-point systematic uncertainties of $< 5\%$. This will allow a precision test of the energy dependence and the angular dependence of scaling behavior of these fundamental cross sections. The proposed experiment requires the standard Hall C equipment which are part of the upgrade and an aerogel Cerenkov detector in the SHMS.

5 The Experiment

5.1 Overview

The experiment will employ the 15 cm Hall C cryogenic liquid hydrogen and deuterium targets, along with the Hall C 6% radiation length copper radiator. The maximum energy of the bremsstrahlung beam is essentially equal to the electron energy. The target, located downstream of the radiator, is irradiated by the photons and the primary electron beam. The kinematics are chosen for the $n(\gamma, \pi^- p)$ (quasifree) and $p(\gamma, \pi^+) n$ processes. The

singles $p(\gamma,\pi^+)n$ measurement will be performed using the HMS and SHMS to detect the π^+, such that we can cover two different center-of-mass angles simultaneously. For cross check, at each energy setting there will be at least one kinematic setting where HMS and SHMS will collect data at the same center-of-mass angle. The coincidence $n(\gamma,\pi^-p)$ measurement will be performed using the HMS as the π^- detector, and the SHMS as the proton detector. The PID requirements of this experiment include the high pressure gas Cerenkov detector which is part of the standard package and an aerogel detectors which is not part of the baseline equipment but is being planned. At each setting data will also be collected with the radiator removed from the beampath. This data will be used to subtract the virtual photon contribution from the primary electron beam.

The $\gamma N \rightarrow \pi N'$ reactions are two-body processes. Thus by either detecting the momentum and the angle of the outgoing nucleon or detecting the momentum and angle of the photo-produced pion, one can determine the incident photon energy. In this experiment for the $n(\gamma,\pi^-p)$ process, a deuterium target will be employed instead of a free neutron target which does not exist in nature. Thus, measurement of the momenta and scattering angles of both the proton and the pion are necessary in order to reconstruct the incident photon energy. Other inelastic channel, such as 2π production can be essentially eliminated, since this is a coincidence measurement and only the highest energy protons and pions are detected. This technique has been well established in experiment E94-104 which was completed in Hall A. Using the data from E94-104, we have compared the reconstructed photon energy spectrum for a ^{2}H target with Monte Carlo simulation of the same (Fig 3). The excellent agreement between the two gives us added confidence in this technique.

5.2 The Electron Beam and the Radiator

An electron beam with a beam current of 50 μA is required for this experiment. The experiment will use a copper radiator of 6% radiation length, which is placed upstream of the target chamber. The copper radiator is a standard Hall-C equipment.

The proposed running conditions of this experiment can be extrapolated from those of E94-104 running conditions, the background from the copper radiator due to the production of low energy neutrons and high energy pions were demonstrated not to be a problem by E94-104. Another experiment, E00-107 which proposes to use a 50 μA beam was approved by the PAC.

5.3 Target

We plan to use the Hall C liquid deuterium, liquid hydrogen (2% r.l. each) cryotargets. The liquid hydrogen target will be used for the singles $\gamma p \rightarrow \pi^+ n$ measurement and for coincidence background studies. The dummy target cell will be used for singles background studies. We propose to run the experiment at a maximum electron beam current of 50 μA, which is significantly below the heat load that the Hall C cryotarget routinely handles. The energy deposited at the highest energy (11.0 GeV) with 50 μA of beam is below the 100 Watts equivalent thick target power limit.

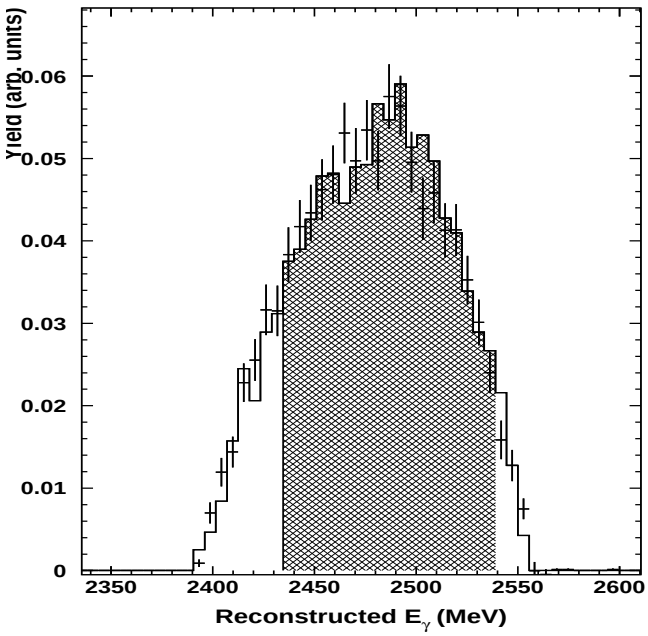

Figure 3: [Reconstructed photon energy spectrum at 2.56 GeV and $\theta_{cm} = 90°$ for a ^{2}H target. The curve is from the Monte Carlo simulation. The shaded area denotes the photon energy region which is used to extract the experimental yield.

5.4 Spectrometer

For the $p(\gamma, \pi^+)n$ processes, the HMS and SHMS will be used simultaneously to detect the π^+. The maximum rates in the spectrometers will be less than 10KHz and thus well below the rate limits for the spectrometer. For the $n(\gamma, \pi^-)p$ process, the HMS-SHMS spectrometer pair will be used to make the coincidence measurement. The HMS will be used for the π^- detection, and the SHMS for the proton detection for most of the experiment, however for the backward angle measurements ($\theta_{CM} > 110^o$) the role of the spectrometers will be switched. The pion arm momentum setting ranges from 0.746 - 10.224 GeV/c and the angle ranges from 6.22 - 87.39°. The proton arm momentum and angle setting ranges from 0.859 - 10.661 GeV/c and 5.97 - 64.76°. These momentum and angular ranges fall well within the limits of the pair of spectrometers when set to detect for the appropriate particle. The total singles rates in each spectrometer is well below 1 MHz in all settings except for the most forward C.M. angle setting. The beam current for these setting has been adjusted such that the highest singles rate in the spectrometer is less than 1 MHz, which is still below the trigger rate limits for the spectrometers.

5.5 Background

The dominant background process for this experiment is the quasi-elastic A(e,e'p) reaction. The quasielastically scattered electron has nearly the same momentum and angle as the photo-produced pion in the pion arm, and the scattered proton also has nearly the same momentum and scattering angle as that of the photo-proton in the proton spec-

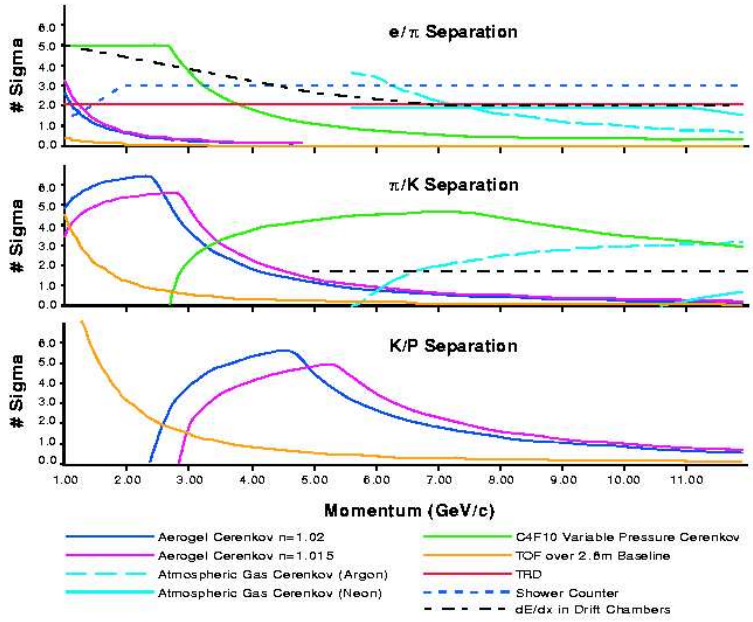

Figure 4: The expected PID with HMS and SHMS detectors.

trometer. We have estimated the singles rates of p and π^+ and the e^- and π^- for the LD2 target, based on the observed rates at lower energies and estimates using the Wiser parametrization [62] and QFS [63] for electrons. The combination of the gas Cerenkov counter, preshower and shower counters can provide an electron rejection factor of 5000, which is sufficient for the proposed experiment. In the proton arm, good particle identification of protons, π^+ particles and positrons is required. The positron background arises from pair production of the bremsstrahlung photons and can be rejected sufficiently using the gas Cerenkov counter because the rate has been estimated to be rather low. Although the π^+ particles from the $\gamma p \rightarrow \pi^+ n$ reactions are kinematically eliminated in the proton arm, the π^+ background event can come from multiple processes, which have relatively low rates because of the phase space constraint. The aerogel detector will provide more than sufficient π^+ and K^+ rejection.

Furthermore, the coincidence requirement effectively suppresses all background channels, except the (e,e'p) channel. Experiment E94-104 demonstrated that the coincidence (e,e'p) background events are sufficiently rejected with the particle identification capabilities provided by the expected detector performance shown in Fig. 4.

5.6 Kinematics

Tables 1 and 2 shows the kinematics for the $p(\gamma, \pi^+)n$ and and the quasifree $n(\gamma, \pi^- p)$ reactions respectively. The photon energy is taken to be 75 MeV below the electron beam energy, since the range of photon energies to be used is a 100 MeV bin from 25 MeV below the end point energy to 125 MeV below the end point energy. The kinematics have been chosen to cover the region between center-of-mass energy $\sqrt{s}$ = 3.0 - 4.62 GeV.

E_{beam}	E_γ	$\sqrt{s}$	θ_{CM}	θ_{π^+} (lab)	P_{π^+}	Spectrometer
GeV	GeV	GeV	deg	deg	GeV/c	
4.4	4.325	3.00	50	67.22	1.121	HMS
			70	47.89	1.709	HMS
			90	34.60	2.376	HMS
			110	24.63	3.042	HMS,SHMS
			130	16.55	3.627	SHMS
			150	9.56	4.062	SHMS
6.6	6.525	3.62	30	87.35	0.844	HMS
			50	57.77	1.528	HMS
			70	40.44	2.444	HMS
			90	28.96	3.484	HMS
			110	20.51	4.524	HMS,SHMS
			130	13.75	5.438	SHMS
			150	7.93	6.116	SHMS
8.8	8.725	4.15	30	79.68	1.000	HMS
			50	51.45	1.928	HMS
			70	35.65	3.173	HMS
			90	25.40	4.588	HMS
			110	17.95	6.003	HMS,SHMS
			130	12.01	7.247	SHMS
			150	6.92	8.170	SHMS
11.0	10.925	4.62	30	73.78	1.153	HMS
			50	46.85	2.325	HMS
			70	32.24	3.901	HMS
			90	22.90	5.691	HMS
			110	16.15	7.481	HMS,SHMS
			130	10.80	9.055	SHMS
			150	6.22	10.223	SHMS

Table 1: Table of kinematics for the $p(\gamma, \pi^+)n$ reaction at pion C.M. angle $30 \leq \theta_{CM} \leq 150$. The photon energy listed is 75 MeV less than the electron beam energy.

E_{beam}	E_γ	$\sqrt{s}$	θ_{CM}	θ_{π^-} (lab)	θ_p (lab)	P_{π^-}	P_p
4.40	4.325	3.0	50.0	67.25	14.89	1.122	4.026
			70.0	47.91	21.76	1.710	3.423
			90.0	34.62	29.68	2.377	2.727
			110.0	24.64	39.14	3.043	2.010
			130.0	16.56	50.69	3.629	1.337
			150.0	9.56	64.76	4.063	0.746
6.60	6.525	3.62	30	87.39	7.41	0.845	6.541
			50	57.80	12.76	1.528	5.855
			70	40.46	18.78	2.445	4.927
			90	28.97	25.90	3.485	3.864
			110	20.52	34.74	4.525	2.784
			130	13.76	46.16	5.439	1.793
			150	7.93	61.10	6.118	0.964
8.80	8.725	4.15	30	79.72	6.57	1.001	8.603
			50	51.48	11.34	1.929	7.674
			70	35.67	16.76	3.174	6.419
			90	25.42	23.27	4.589	4.986
			110	17.96	31.56	6.004	3.537
			130	12.02	42.69	7.248	2.226
			150	6.92	58.08	8.171	1.160
11.0	10.925	4.62	30	73.81	5.97	1.154	10.661
			50	46.87	10.31	2.326	9.488
			70	32.26	15.28	3.902	7.905
			90	22.91	21.31	5.692	6.099
			110	16.16	29.12	7.482	4.280
			130	10.81	39.91	9.056	2.646
			150	6.22	55.52	10.224	1.344

Table 2: Table of kinematics for the quasifree $n(\gamma, \pi^- p)$ reaction at pion C.M. angle $30^o \leq \theta_{CM} \leq 150^o$. The photon energy listed is 75 MeV less than the electron beam energy.

The electron energy were chosen such that a single linac energy is needed for the entire experiment.

5.7 Counting Rates

The counting rate were estimated using the cross-section measured by experiment E94-104 at 90^o C.M. angle, at the highest $\sqrt{s}$ covered in that experiment. We assumed the cross-section scales as s^{-7} for the energy dependence and the angular dependence was taken to be $\frac{1}{(1+\cos\theta_{CM})^4} \cdot \frac{1}{(1-\cos\theta_{CM})^5}$ [1]. All rates were estimated for a 100 MeV photon energy window starting 25 MeV below the end point energy. A maximum beam current of 50 μA and a 6% copper radiator was used in the estimation.

The estimated counting rates are shown below in Table 3

The singles $d(\gamma, \pi^-)$, $d(\gamma, p)$ and $d(\gamma, \pi^+)$rates and the singles $d(e, \pi^-)$, $d(e, p)$ and $d(e, \pi^+)$ rates were estimated using the parametrization of SLAC data of Wiser *et al.* [62]. The e^- singles rates were estimated using the code QFS [63]. The singles rates and the e^-/π^- ratio for the LD2 targets is shown in Tables 4 and 5.

5.8 Beam Time Estimate

Beam times requirements for data with the radiator were estimated for a goal of 3% statistical uncertainty for the LH2 and LD2 targets. The beam time estimates for the data without the radiator are taken to be a third of the time required with the radiator. The beam time estimates are shown below in table 6. It includes 20 hours of background studies for the coincidence measurement and 12 hours of background studies for the singles measurement. In addition to the 172 hours of beam time listed in the table, we estimate the time for beam energy change [64] for the 4 kinematic points (3 changes) to be an average of 6 hrs each. Thus the total overhead for beam energy and target change is expected to be around 18 hours. The spectrometer momentum and angle settings will have to be changed a total of 48 times these changes have been assigned a time of 1 hr each change. Thus a total of $\sim$ 50 hours of overhead will be required for the spectrometer changes. The total overhead is expected to be 68 hours and the total time required for the experiment is 240 hours (10 days).

5.9 Systematic Uncertainties and Projected Results

The experience gained in E94-104 suggests that the systematic uncertainties of this kind of experiment are well under control. For the cross-section measurements the systematic uncertainties are expected to be $< 8\%$. However, the systematic uncertainty in energy dependence of the cross-section will be $< 5\%$. The projected results for LH2 and LD2 targets are shown in Fig. 5 and Fig. 6. The J/Ψ threshold is also indicated in these figures. There is ample coverage on both sides of the threshold. Fig. 7 shows the projected angular coverage at C.M. energy $\sqrt{s} > 4.62$ GeV. Thus this experiment will provide angular as well as energy scan of pion photo-production cross-section which will allow us to explore the scaling behavior of the cross-section in great detail. Fig. 8 show the projected π^-/π^+ ratio as function of momentum transfer $|t|$ at C.M. angle of 90°.

E_{beam}	$\sqrt{s}$	θ_{CM}	Current	LH2 rates(HMS)	LD2 rates
GeV	GeV	deg	μA	Hz	Hz
4.40	3.0	50	30	112.7	86.0
		70	50	12.7	9.7
		90	50	5.2	4.0
		110	50	6.5	5.0
		130	50	27.7	21.1
		150	50	743.9	569.7
6.60	3.62	30	20	349.6	266.9
		50	50	12.0	9.2
		70	50	1.3	1.0
		90	50	0.6	0.4
		110	50	0.7	0.5
		130	50	2.9	2.2
		150	50	76.7	58.6
8.80	4.15	30	35	121.4	92.7
		50	50	2.4	1.8
		70	50	0.3	0.2
		90	50	0.1	0.1
		110	50	0.1	0.1
		130	50	0.6	0.4
		150	50	14.8	11.3
11.0	4.62	30	50	48.7	37.2
		50	50	0.7	0.5
		70	50	0.1	0.05
		90	50	0.03	0.02
		110	50	0.04	0.03
		130	50	0.2	0.1
		150	50	4.1	3.1

Table 3: Estimated rates for LH2 (singles), LD2 (coincidence) in a 100 MeV photon energy window starting 25 MeV below the end point energy.

$\sqrt{s}$	θ_{CM}	$d(\gamma,p)$ rates	$d(e^-,p)$ rates	$d(\gamma,pi^+)$ rates	$d(e,pi^+)$ rates
GeV	(deg)	Hz	Hz	Hz	Hz
3.0	50	45986.1	15041.1	1713.5	482.4
	70	25808.2	6714.6	531.2	127.3
	90	16822.4	3632.3	229.6	43.8
	110	18959.0	3602.6	273.9	38.5
	130	19910.7	18207.3	964.5	90.3
	150	19675.9	51373.8	9056.5	472.9
3.62	30	49855.2	59845.2	1790.0	819.6
	50	14816.9	6313.7	273.8	112.2
	70	3449.2	1234.9	35.5	12.2
	90	2071.4	600.8	13.1	3.5
	110	2435.3	594.7	16.5	3.2
	130	1838.1	1180.0	79.8	10.0
	150	6723.8	22686.0	1372.7	92.6
4.15	30	34908.2	24293.8	766.8	461.7
	50	3518.1	1925.1	43.6	23.4
	70	566.5	261.2	4.2	1.9
	90	285.5	105.6	1.4	0.5
	110	336.1	103.9	1.8	0.5
	130	32.3	251.5	11.4	1.8
	150	4682.8	19012.2	316.1	25.7
4.62	30	21722.1	16978.9	337.7	252.0
	50	961.3	646.7	9.3	6.2
	70	104.8	59.8	0.7	0.4
	90	47.0	21.5	0.2	0.1
	110	50.1	20.9	0.3	0.1
	130	8.5	79.1	2.3	0.4
	150	2804.0	13190.1	92.7	8.7

Table 4: Estimated singles rates in the p spectrometer, for an LD2 target in a 100 MeV photon energy window starting 25 MeV below the end point energy.

$\sqrt{s}$	θ_{CM}	$d(\gamma,\pi^-)$ rates	$d(e^-,\pi^-)$ rates	e^-/π^-
GeV	(deg)	Hz	Hz	
3.0	50	3.15	20.0	0.17
	70	1.01	4.38	0.54
	90	1.0	3.63	2.90
	110	1.82	6.5	24.92
	130	12.83	30.5	363.02
3.62	30	12.85	144.8	0.004
	50	1.36	9.80	0.02
	70	0.41	1.97	0.09
	90	0.49	1.80	0.69
	110	1.33	4.52	7.42
	130	30.42	72.36	79.94
	150	261.71	712.75	2829.77
4.15	30	5.07	83.71	0.001
	50	0.33	3.06	0.003
	70	0.09	0.57	0.023
	90	0.09	0.40	0.19
	110	0.30	1.12	2.31
	130	2.40	8.40	28.76
	150	4.641	18.42	132.1
4.62	30	1.22	29.91	0.0001
	50	0.048	0.62	0.0009
	70	0.01	0.07	0.006
	90	0.01	0.05	0.058
	110	0.02	0.11	0.45
	130	0.28	1.46	10.76
	150	10.53	54.86	649.89

Table 5: Estimated singles rates in the π^- spectrometer, for an LD2 target in a 100 MeV photon energy window starting 25 MeV below the end point energy.

$\sqrt{s}$	θ_{CM}	LH2 beam time	LD2 beam time	Total
GeV	deg	hours	hours	hours
3.0	50	0.5	0.5	1.0
	70	0.5	0.5	1.0
	90	0.5	0.5	1.0
	110	0.5	0.5	1.0
s	130	0.5	0.5	1.0
s	150	0.5	0.5	1.0
3.62	30	0.5	0.5	1.0
	50	0.5	0.5	1.0
	70	0.5	0.5	1.0
	90	1.0	1.0	2.0
	110	0.5	1.0	2.0
s	130	0.5	0.5	1.0
s	150	0.5	0.5	1.0
4.15	30	0.5	0.5	1.0
	50	0.5	0.5	1.0
	70	1.5	2.0	3.5
	90	3.0	4.0	7.0
	110	2.5	4.0	9.0
s	130	2.0	1.0	3.0
s	150	0.5	0.5	1.0
4.62	30	0.5	0.5	1.0
	50	0.5	1.0	1.5
	70	4.5	6.0	10.5
	90	11.5	14.0	24.0
	110	9.0	11.5	20.5
s	130	4.0	3.0	7.0
s	150	0.5	0.5	1.0
Radiator IN		48	57	105
Radiator OUT		16	19	35
Bgd Studies		12	20	32
Total				172
Overhead				18+50
Grand Total		73	99	240 (10.0 days)

Table 6: Estimated beam time requirements. The angles marked with "s" will collect data simultaneously with other settings, but only for the LH2 target.

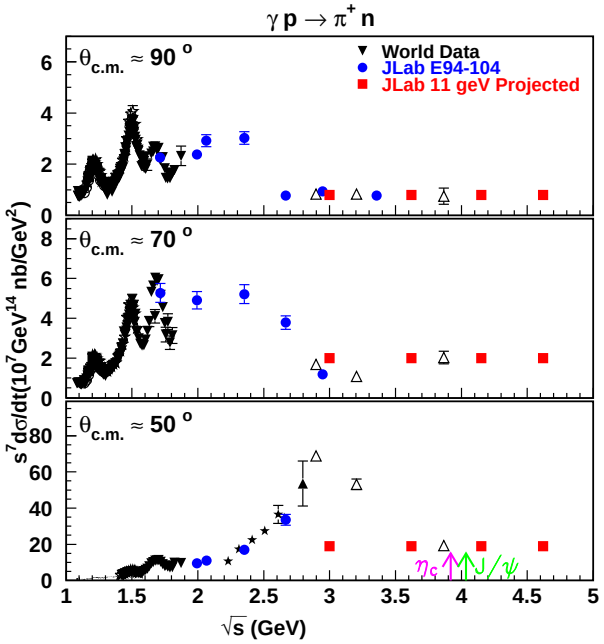

Figure 5: The projected measurement (red solid points) for the scaled differential cross-section for the process $p(\gamma, \pi^+)n$ as a function of cms energy $\sqrt{s}$ in GeV for 3 different C.M. angles. A 3% statistical uncertainty and a point-to-point 5% systematic uncertainty added in quadrature is shown in the projection.

6 Collaboration Background and Responsibilities

Many members of the current collaboration have been involved in a number of bremsstrahlung photon beam experiments at SLAC and JLab. Most members of the group are experienced in running the Hall-C radiator, cryotargets and spectrometers. This experiment is a natural continuation of the experiment E94-104 and most members have participated in that experiment as well as other JLab photo-proton polarization experiments (E89-019 and E94-012).

7 Acknowledgments

We thank G.A. Miller, M. Sargsian and T. W. Donnelly for helpful comments.

References

[1] R.L. Anderson *et al.*, Phys. Rev. **D14**, 679 (1976).

[2] C. White *et al.*, Phys. Rev. **D49**, 58 (1994).

[3] S.J. Brodsky and G.R. Farrar, Phys. Rev. Lett.**31**, 1153 (1973); Phys. Rev. D **11**, 1309 (1975); V. Matveev *et al.*, Nuovo Cimento Lett. **7**, 719 (1973);

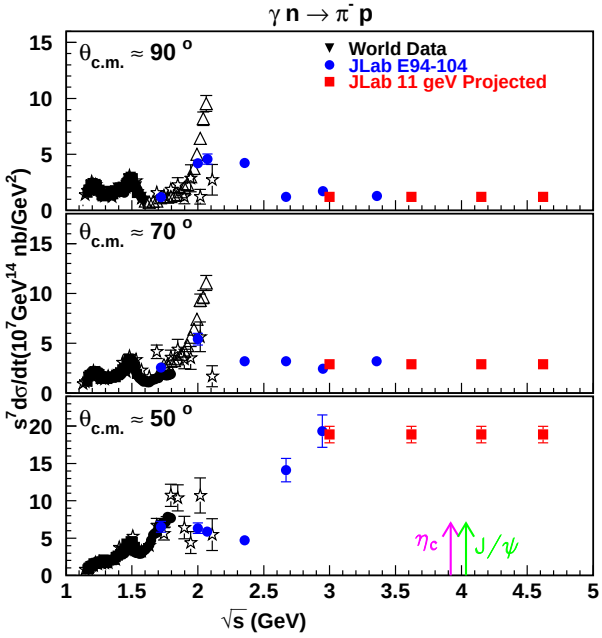

Figure 6: The projected measurement (red solid points) for the scaled differential cross-section for the process $n(\gamma, \pi^- p)$ as a function of cms energy $\sqrt{s}$ in GeV for 3 different C.M. angles. A 3% statistical uncertainty and a point-to-point 5% systematic uncertainty added in quadrature is shown in the projection.

[4] G.P. Lepage, and S.J. Brodsky, Phys. Rev. D **22**, 2157 (1980).

[5] T. Gousset, B. Pire and J. P. Ralston, Phys. Rev. D **53**, 1202 (1996).

[6] N. Isgur and C. Llewelyn-Smith, Phys. Rev. Lett. **52**, 1080 (1984).

[7] X. Ji, J.-P. Ma and F. Yuan, Phys. Rev. Lett. **90**, 241601 (2003).

[8] J. Polchinski and M.J. Strassler, Phys. Rev. Lett. **88**, 031601 (2002); R.C. Brower and C.I. Tan, Nucl. Phys. B **662**, 393 (2003); O. Andreev, Phys. Rev. D **67**, 046001 (2003).

[9] S. J. Brodsky and G. F. de Teramond, Phys. Lett. **B582**, 211 (2004); S. J. Brodsky *et al.*, Phys. Rev. D **69**, 076001 (2004).

[10] J. Napolitano *et al.*, Phys. Rev. Lett. **61**, 2530 (1988); S.J. Freedman *et al.*, Phys. Rev. C **48**, 1864 (1993); J.E. Belz *et al.*, Phys. Rev. Lett. **74**, 646 (1995).

[11] C. Bochna *et al.*, Phys. Rev. Lett. **81**, 4576 (1998).

[12] E.C. Schulte, *et al.*, Phys. Rev. Lett. **87**, 102302 (2001);

[13] P. Rossi *et al.*, hep-ph/0405207, submitted to Phys. Rev. Letts.; M. Mirazita *et al.*, Phys. Rev. C **70**, 014005 (2004).

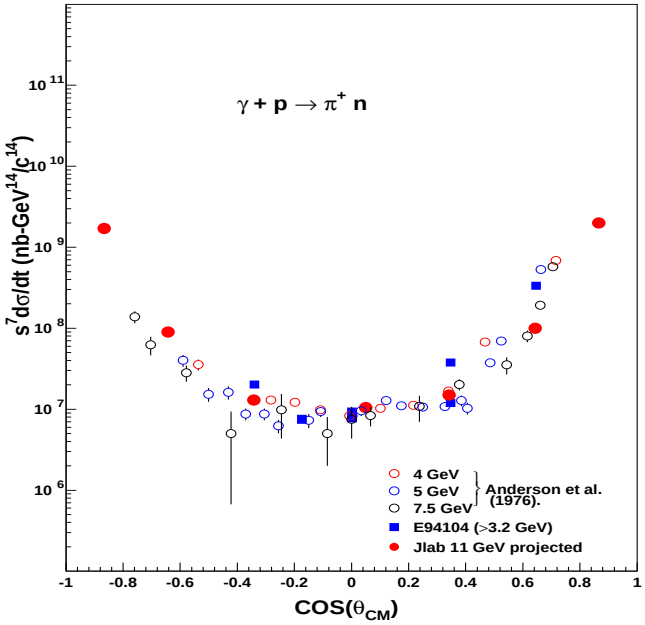

Figure 7: The scaled cross-section $s^7 \frac{d\sigma}{dt}$ for the $p(\gamma, \pi^+)n$ process as a function of $\cos(\theta_{CM})$. The soild red points are the projected angular coverage at C.M. energy of $\sqrt{s}$= 4.62 GeV.The experiment will have a similar angular coverage for both $p(\gamma, \pi^+)n$ and the $n(\gamma, \pi^- p)$ processes, over the entire energy range proposed.

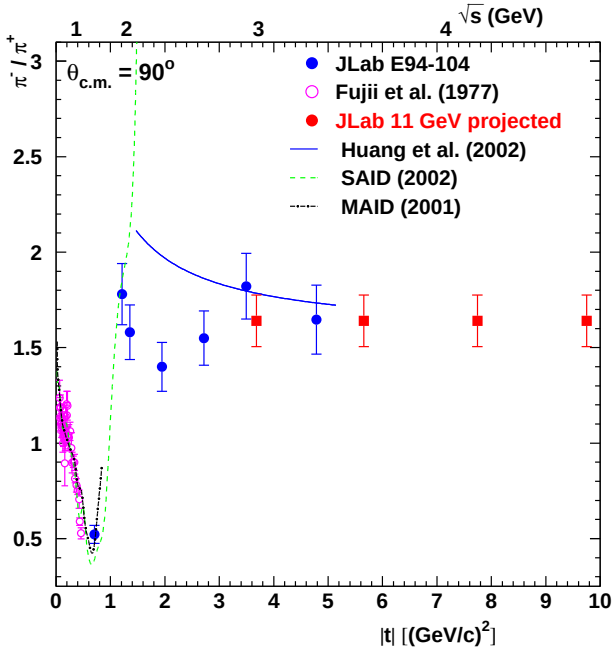

Figure 8: The projected π^-/π^+ ratio as function of energy at C.M. angle of 90°.

[14] K. Wijesooriya, *et al.*, JournalPhys. Rev. Lett.86, 2975 (2001).

[15] K. Wijesooriya, *et al.*, JournalPhys. Rev. C66, 034614 (2002).

[16] D. P. Owen *et al.*, Phys. Rev. **181**, 1794 (1969); K. A. Jenkins *et al.*, Phys. Rev. D **21**, 2445 (1980); C. Haglin *et al.*, Nucl. Phys. B **216**, 1 (1983).

[17] "Photoproduction of Elementary Particles", edited by H. Genzel, P. Joos and W. Pfeil pp16-268, (1973).

[18] L. Y. Zhu *et al.*, Phys. Rev. Lett. **91**, 022003 (2003); L. Y. Zhu *et al.*, nucl-exp/0409018.

[19] S. J. Brodsky, and G. F. de Teramond, Phys. Rev. Lett. **60**, 1924 (1988).

[20] O. Bartholomy *et al.*, Phys. Rev. Lett. **94**,012003 (2005).

[21] H.-J. Besch *et al.*, Z. Phys. C **16**, 1 (1982).

[22] I. I. Strakovsky (private communication); R. A. Arndt *et al.*, Phys. Rev. **C66**, 055213 (2002); nucl-th/0205067; http://gwdac.phys.gwu.edu/.

[23] I. I. Strakovsky (private communication); S. S. Kamalov, *et al.*, Phys. Rev. C **64**, 032201 (2001)(A dynamical model); D. Drechsel, *et al.*, Nucl. Phys. A **645**, 145 (1999)(a unitary isobar model); MAID2001 refers to the Nov. 2001 version of the MAID solution from S. S. Kamalov.

[24] H. W. Huang (private communication); H. W. Huang and P. Kroll, Eur. Phys. J. C **17**, 423 (2000); P. Kroll, hep-ph/0207118, (2002); A. Afanasev, C. E. Carlson, and C. Wahlquist, Phys. Lett. B **398**, 393 (1997).

[25] H.W. Huang *et al.*, hep-ph/0309071.

[26] D. Dutta *et al.*, Phys. Rev. C **68**, 021001 (2003).

[27] P. V. Landshoff, Phys. Rev. D **10**, 1024 (1974).

[28] A.W. Hendry, Phys. Rev. D **10**, 2300 (1974).

[29] D.G. Crabb *et al.*, Phys. Rev. Lett. **41**, 1257 (1978).

[30] G.R. Court *et al.*, Phys. Rev. Lett. **57**, 507 (1986), T.S. Bhatia *et al.*, Phys. Rev. Lett. **49**, 1135 (1982), E.A. Crosbie *et al.*, Phys. Rev. D **23**, 600 (1981).

[31] S.J. Brodsky, C.E. Carlson, and H. Lipkin, Phys. Rev. D **20**, 2278 (1979).

[32] A. Sen, Phys. Rev. D **28**, 860 (1983).

[33] J. Botts and G. Sterman, Nucl. Phys. **B325**, 62 (1989).

[34] A. H. Mueller, Phys. Rep. **73**, 237 (1981).

[35] A.S. Carroll *et al.*, Phys. Rev. Lett. **61**, 1698 (1988).

[36] Y. Mardor *et al.*, Phys. Rev. Lett. **81**, 5085 (1998); A. Leksanov *et al.*, Phys. Rev. Lett. **87**, 212301-1 (2001).

[37] J.P. Ralston and B. Pire, Phys. Rev. Lett. **61**, 1823 (1988), J.P. Ralston and B. Pire, Phys. Rev. Lett. **65**, 2343 (1990).

[38] C.E. Carlson, M. Chachkhunashvili, and F. Myhrer, Phys. Rev. D **46**, 2891 (1992).

[39] Q. Zhao and F. E. Close, Phys. Rev. Lett. **91**, 022004 (2003).

[40] A. V. Belitski, X. Ji and F. Yuan, Phys. Rev. Lett. **91**, 092003 (2003).

[41] M. K. Jones *et al.*, Phys. Rev. Lett. **84**, 1398 (2000); O. Gayou *et al.*, Phys. Rev. Lett. **88**, 092301 (2002).

[42] D. Dutta and H. Gao, Phys. Rev. C. **71**, 032201R (2005).

[43] C. W. Akerlof, *et al.*, Phys. Rev. 159, 1138 (1967); R. C. Kammerud, *et al.*, Phys Rev. D **4**, 1309 (1971); K. A. Jenkins, *et al.*, Phys. Rev. Lett, **40**, 425 (1978).

[44] L.L. Frankfurt, G.A. Miller, M.M. Sargsian, and M.I. Strikman, Phys. Rev. Lett. **84**, 3045 (2000), M.M. Sargsian, private communication.

[45] P. Jain, B. Kundu, and J. Ralston, Phys. Rev. D **65**, 094027 (2002).

[46] G.R. Farrar, G. Sterman, and H. Zhang, Phys. Rev. Lett. **62**, 2229 (1989).

[47] E. Anciant *et al.*, Phys. Rev. Lett. **85**, 4682 (2000).

[48] B. Kundu, J. Samuelsson, P. Jain and J.P. Ralston, Phys. Rev. D **62**, 113009 (2000).

[49] S.J. Brodsky and A.H. Mueller, Phys. Lett. **B 206**, 685 (1988).

[50] G.R. Farrar, H. Liu, L.L. Frankfurt, and M.I. Strikman, Phys. Rev. Lett. **61**, 686 (1988).

[51] P. Jain, B. Pire, and J.P. Ralston, Phys. Rep. **271**, 67 (1996).

[52] N.C.R. Makins *et al.*, Phys. Rev. Lett. **72**, 1986 (1994); T.G. O'Neill *et al.*, Phys. Lett. **351**, 87 (1995); D. Abbott, *et al.*, Phys. Rev. Lett. **80**, 5072 (1998); K. Garrow, *et al.*, Submitted to Phys. Rev. C.

[53] P. Jain, private communication.

[54] A. Arriaga, V. R. Pandharipande and R. B. Wiringa, Phys. Rev. C **52**,2362 (1995).

[55] H. Gao, R. J. Holt and V. R. Pandharipande, Phys. Rev. C **54**, 2779 (1996).

[56] R. J. Glauber, in *Lectures in Theoretical Physics*,edited by W. E. Brittin *et al.*, (Interscience, New York, 1959).

[57] S. Liuti and S. K. Taneja, hep-ph/0405014.

[58] X. Ji, Phys. Rev. Lett. **78**, 610 (1997); Phys. Rev. D **55**, 7114 (1997); A.V. Radyushkin, Phys. Lett, **B380**, 417 (1996); Phys. Rev. D **56**, 5524 (1997).

[59] M. Burkardt and G. A. Miller, hep-ph/0312190.

[60] M. Burkardt, Int J.. Mod. Phys. A **18**, 173 (2003).

[61] D. Dutta, Ph.D. Thesis, Northwestern University, Unpublished, (1999).

[62] L. W. Whitlow, SLAC-Report-357,(1990); D. E .Wiser, Ph. D. Thesis, University of Wisconsin (1977); P. Bosted private communication.

[63] J. W. Lightbody Jr. and J. S. O'Connell, NBS

[64] H. Areti, private communication.

[65] M. A. Shupe *et al.*, Phys. Rev. D. **19**, 1921 (1979).